Thermal Neutron Scattering Law Data Evaluations for Nuclear Technology Applications

Ayman I. Hawari, Yuwei Zhu, Jonathan L. Wormald, Cole A. Manring, Nina Colby Sorrell

Department of Nuclear Engineering, North Carolina State University, Raleigh, North Carolina 27695, USA
ayman.hawari@ncsu.edu

Abstract – *Thermal neutron scattering law (TSL) data have been produced for various materials of interest in nuclear technology applications (e.g., nuclear reactor design and criticality safety analysis). Evaluations were performed for polymethylmethacrylate (Lucite), polyethylene and heavy paraffinic oils. In addition, updated evaluations for beryllium, beryllium oxide, graphite, and a new evaluation for "nuclear" graphite were produced. The evaluations applied the incoherent approximation of thermal neutron scattering theory. However, in some cases corrections accounting for incoherent inelastic scattering effects were included through the use of a recently developed computational nuclear data evaluation platform (FLASSH). All evaluations were produced in the ENDF File 7 format.*

I. INTRODUCTION

In various nuclear technology systems, neutrons are generated at high energy and moderate to slow down until reaching the thermal range. In this range, neutrons exchange energy with the atoms of a medium through inelastic scattering reactions with the atomic lattice until eventually attaining a quasi-equilibrium energy spectrum that is described by the conditions of the medium including its temperature and the details of its structure and dynamics. Quantitatively, thermal inelastic scattering may be described using Born scattering theory combined with a nuclear pseudopotential that was proposed by Fermi [1]. The double differential scattering cross section for this process is given by

$$\frac{\partial^2 \sigma}{\partial \Omega \partial E'} = \frac{1}{4\pi}\sqrt{\frac{E'}{E}}\left[\sigma_{coh}S(\alpha,\beta)+\sigma_{inc}S_s(\alpha,\beta)\right], \quad (1)$$

where E is the incident energy of the neutron, E' is the outgoing energy, Ω is the scattering solid angle, σ represents the bound atom coherent and incoherent scattering cross sections, respectively, S is the thermal scattering law (TSL), and S_s is the self (noninterference) component of the scattering law. In this notation, α is the dimensionless momentum transfer variable and β is the dimensionless energy transfer variable.

Due to recent developments in the utilization of atomistic simulation techniques (e.g., *ab initio* density functional theory and molecular dynamics based methods), and in using more complete treatment of scattering theory [2], the ability to readily generate the TSL for various materials of interest to nuclear technology applications (e.g., nuclear reactor design, criticality safety analysis, neutron beam spectral shaping, etc.) has become possible. In this work, new and updated TSL data and the resulting inelastic scattering cross sections are presented for a set of materials that represent moderators and reflectors that are important for neutronic systems such as thermal nuclear reactors.

II. ATOMISTIC SIMULATION METHODS

The fundamental data that is required to generate the TSL is obtained using atomistic *ab initio* density functional theory (DFT) and classical molecular dynamics (MD) simulations. These techniques are based on the adiabatic approximation, which considers the electronic and nuclear components of an atomic system separately. DFT based methods are combined with the dynamical matrix approach to generate the phonon density of states (DOS) for use in TSL calculations. Alternatively, MD methods are used to calculate atomic trajectories and generate the velocity autocorrelation function from which the DOS can be obtained as its power spectrum.

While DFT analysis is quantum mechanical in nature and does not assume a specific atomic force field for a given material, classical MD methods require the assumption of a semi-empirical potential function for the atomic system. In this case, the potential function is parametrized to capture the fundamental properties (e.g., density, thermal expansion, thermal conductivity, etc.) of the material, and subsequently applied in DOS calculations. However, it should be noted that MD analysis is inherently capable of accounting for the temperature of the medium, while DFT (lattice dynamics) analysis is valid only at low temperatures.

III. THERMAL SCATTERING LAW DATA GENERATION

The TSL and the resulting thermal scattering cross sections are calculated using Eq. 1 and under primarily the incoherent approximation, where S is assumed to be completely represented by S_s. This reduces Eq. 1 to the following expression

$$\frac{\partial^2 \sigma}{\partial \Omega \partial E'} = \frac{1}{4\pi}\sqrt{\frac{E'}{E}}\left[(\sigma_{coh}+\sigma_{inc})S_s(\alpha,\beta)\right]. \quad (2)$$

The generation of the TSL and the scattering cross sections was performed using the LEAPR and THERMR

modules of the NJOY code system under the incoherent approximation, where Eq. 2 is implemented [3,4]. TSL generation was also investigated using a recently developed code system (Full Law Analysis Scattering System Hub, FLASSH) that is capable of relaxing all the primary approximations of NJOY (i.e., incoherent approximation, short collision time approximation, cubic approximation, atom site approximation, etc.) [5,6]. In this case, Eq. 1 is implemented using a correction accounting for coherent inelastic scattering effects. As a result, for crystalline materials where harmonic atomic forces are assumed, the typically applied "phonon expansion" gives the following expression for the inelastic double differential scattering cross section

$$\frac{d^2\sigma}{d\Omega dE'} \cong \frac{1}{4\pi}\sqrt{\frac{E'}{E}}\left\{(\sigma_{coh}+\sigma_{incoh})\left(\sum_{P=2}{}^{P}S_s\right)_{incoh} + \sigma_{coh}\left({}^1S_s + {}^1S_d\right)_{exact}\right\}, \qquad (3)$$

where P represents the number of phonons created or annihilated in the scattering process. Furthermore, the FLASSH code system includes a generalized coherent elastic scattering module that applies the Debye-Waller matrix approach for generating the coherent elastic cross section for crystalline materials [7].

Below is a description of TSL evaluations that have been performed recently and contributed to the ENDF database for consideration in the upcoming ENDF/B-VIII release. The TSL and thermal scattering cross section libraries are generated in different formats such as the ENDF File 7 format and as ACE continuous energy libraries for use in neutronic simulations.

IV. TSL OF HYDROCARBONS AND POLYMERS

In these materials, the primary scattering species is hydrogen for which incoherent scattering is dominant. Under typical conditions (i.e., room temperature and pressure), polymers are amorphous materials that are represented by monomer building blocks connected in long molecular chains. Alternatively, hydrocarbons, such as paraffinic oils, are usually heavy liquids that are composed of large (e.g., C_nH_{2n+2}) molecules, where n represents the number of atoms.

TSL libraries were generated for hydrogen in the polymers polymethylmethacrylate, $(C_5H_8O_2)_n$, and polyethylene, $(CH_2)_n$, and in paraffinic oil. In all cases, classical molecular dynamics simulations (using the LAMMPS code [8]) were performed to generate the density of states for hydrogen in the atomic system. The Dreiding force field was used to simulate the polymers. The MD simulations were conducted at 300 K and 1 atmosphere pressure using supercells that contain thousands of atoms. In all cases, the models were verified to produce the

materials physical behavior such as density, viscosity, and phase transition prior to proceeding with DOS calculations. A similar approach was used for producing the TSL for the paraffinic oil. In this case, the COMPASS force field was utilized at a similar temperature and pressure. Figure 1 below shows the thermal scattering cross sections for the $(C_5H_8O_2)_n$ and $(CH_2)_n$ polymers, and for the paraffinic oil.

V. TSL OF BERYLLIUM AND BERYLLIUM OXIDE

The TSL for beryllium metal and beryllium oxide were generated using *ab initio* density functional theory methods. This represents a significant improvement over the semi-empirical central force techniques used in past work [3]. In both cases, the phonon DOS was calculated using the force field generated using the VASP code and the solution of the associated dynamical matrix using the PHONON code [9,10,11]. Figure 2 shows the resulting total thermal neutron inelastic cross sections in comparison to current ENDF/B-VII data [12]. As it can be seen, the beryllium data generated in this work shows significantly improved agreement with experimental results.

In addition, the TSL for beryllium was calculated using the FLASSH code [6]. This calculation is based on Eq. 3 and avoids the traditional incoherent approximation (i.e., Eq. 2) as used in the NJOY code. This approach allows generating the TSL as observed experimentally and therefore enables direct comparison of computational and measured results. The required input for generating such data includes the detailed atomic dispersion and polarization information as calculated using the VASP/PHONON code system. The technique is currently being considered for all relevant materials as the path forward for generating TSL libraries that are free from major approximations.

VI. TSL OF NUCLEAR AND IDEAL GRAPHITE

Graphite is a key nuclear material that has been used since the early stages of nuclear technology [13]. Ideal graphite is crystalline and has a highly anisotropic hexagonal structure with greater separation perpendicular to the basal plane. It is composed of ABAB stacked planes of carbon that have strong covalent bonding within the basal plane and weaker Van der Waals bonding between planes. However, "nuclear" graphite represents an artificially manufactured material resulting in a nearly isotropic structure where graphite crystallites are embedded within a homogenous carbon matrix. Nuclear graphite is characterized with densities in the range of 1.5-1.8 g/cm^3 in comparison to a density of 2.25 g/cm^3 for ideal graphite. In addition, a distinguishing feature of nuclear graphite is its porosity that can vary up to nearly 30%.

In this work, TSL libraries for nuclear and ideal graphite have been generated at various temperatures. For ideal graphite, the libraries are based on VASP DFT calculations that produced the intraplanar Hellmann-

Feynman forces and interplanar Van der Waals forces. These forces were then applied to predict the phonon DOS using the dynamical matrix approach as implemented in the PHONON code. For nuclear graphite, the libraries are based on vibrational DOS data that was calculated using MD methods, which shows increased softness in comparison to the ideal graphite DOS. This DOS softening is attributed to porosity effects. The TSL and calculated inelastic cross sections are shown in Fig. 3. For comparison, the total inelastic thermal scattering cross section of nuclear graphite, with 10% porosity levels, is plotted alongside the ideal graphite cross sections showing the enhancement due to porosity. In addition, the nuclear graphite total cross section data shows significantly improved agreement with the measured data as reported in the literature [14,15].

VII. CONCLUSIONS

Thermal neutron scattering law (TSL) libraries were produced for beryllium, beryllium oxide, graphite, nuclear graphite, polymethylmethacrylate (Lucite), polyethylene and heavy paraffinic oils. All libraries were generated in the ENDF File 7 format and contributed for potential inclusion in the upcoming ENDF/B-VIII release. The generation of this data is based on fundamental atomistic simulations that use ab initio DFT and classical MD models to calculate the required atomic and molecular excitation spectra.

The final TSL libraries were produced in the framework of the incoherent approximation and, in certain cases, included corrections for coherent inelastic effects. The ability to include such corrections produces TSL data that show improved agreement with measured results. This is enabled through a new computational platform (FLASSH) that is in its early stages of implementation and is capable of producing TSL libraries that are free form many of the past approximations (incoherent approximation, short collision time approximation, cubic approximation, etc.).

ACKNOWLEDGMENTS

REFERENCES

1. G.L. SQUIRES, *Introduction to The Theory of Thermal Neutron Scattering*, Cambridge University Press, UK (1978).

2. A.I. HAWARI, "Modern Techniques for Inelastic Thermal Neutron Scattering Analysis," *Nucl. Data Sheets*, **118**, 172 (2014).

3. R.E. MACFARLANE, "New Thermal Neutron Scattering Files for ENDF/B-VI, Release 2," LA-12639-MS, Los Alamos National Laboratory (1994).

4. R.E. MACFARLANE et al., "The NJOY Nuclear Data Processing System, Version 2012," LA-UR-12-27079, Los Alamos National Laboratory (2012).

5. A. I. HAWARI, et al., "Graphite Thermal Neutron Scattering Cross Section Calculations Including Coherent 1-Phonon Effects", Proc. PHYSOR 2008, Interlaken, Switzerland, Sept 14-19, (2008).

6. Y. ZHU, A.I. HAWARI, "Full Law Analysis Scattering System Hub (FLASSH)", *Trans. American Nucl. Soc.*, **116**, (2017).

7. Y. ZHU, A.I. HAWARI, "Implementation of a generalized coherent elastic scattering formulation for thermal neutron scattering analysis," Proceedings of ICNC 2015, Sep. 13-17, American Nuclear Society (2015) (CD-ROM).

8. S.J. PLIMPTON, "Fast parallel algorithms for short-range molecular dynamics," *J. Comp. Phys.*, **117**, 1 (1995).

9. G. KRESSE, G. FURTHMÜLLER, "Efficiency of ab-initio total energy calculations for metals and semiconductors using a plane-wave basis set," *Comput. Mat. Sci.*, **6**, 15 (1996).

10. G. KRESSE, G. FURTHMÜLLER, "," Phys. Rev. B **54**, 11169 (1996).

11. K. PARLINSKI et al., "First-Principles Determination of the Soft Mode in Cubic ZrO_2," *Phys. Rev. Lett.*, **78**, 4063 (1997).

12. M.B. CHADWICK et al., "ENDF/B-VII.1 Nuclear Data for Science and Technology: Cross Sections, Covariances, Fission Product Yields and Decay Data," *Nucl. Data Sheets* **112**, 2887 (2011).

13. "The First Reactor," US Department of Energy, DOE/NE-0046 (1982).

14. D.J. HUGHS, R.B. SCHWARTZ, Neutron Cross Sections, BNL-325, Second Edition (1958).

15. A.I. HAWARI et al., "Measurement of The Total Inelastic Scattering Cross Section of Graphite Using 9 Angstrom Neutrons", *Trans. American Nucl. Soc.*, **100**, 591 (2009).

16. G. SIBONA et al., "Thermal Neutron Cross Sections and Diffusion Parameters of Plexiglass," Anna. Nucl. Energy, 18, 689 (1991).

17. K. KANDA and O. AIZAWA, "Effect of temperature on total cross section of beryllium for thermal neutrons," J. Nuclear Science and Technology, 12, 601 (1975).
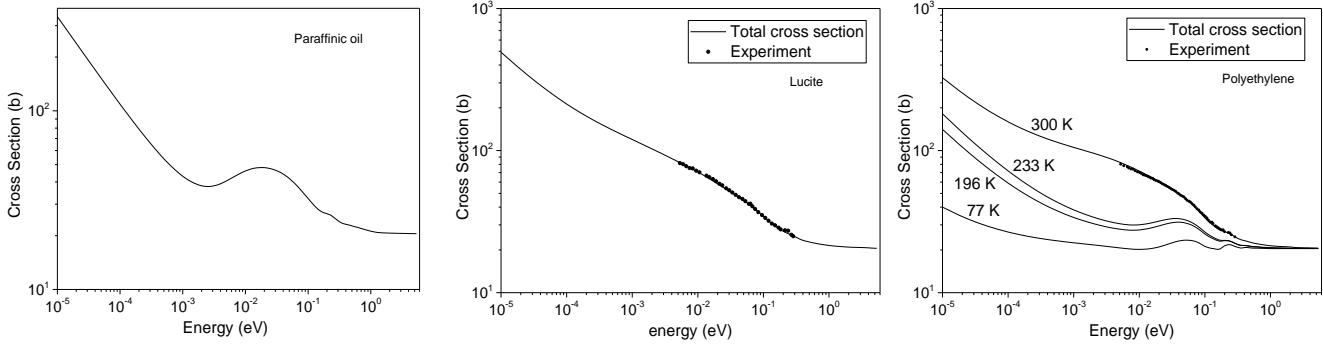
Fig. 1. The thermal scattering cross sections for heavy paraffinic oil (left), and the thermal scattering cross sections for polymethylmethacrylate, $(C_5H_8O_2)_n$, (center), and polyethylene, $(CH_2)_n$, (right). All data is based on classical MD simulations and is generated at a temperature of 300 K and 1 atmosphere. Multiple temperatures are shown for polyethylene. The calculated data shows good agreement with experimental data [16].
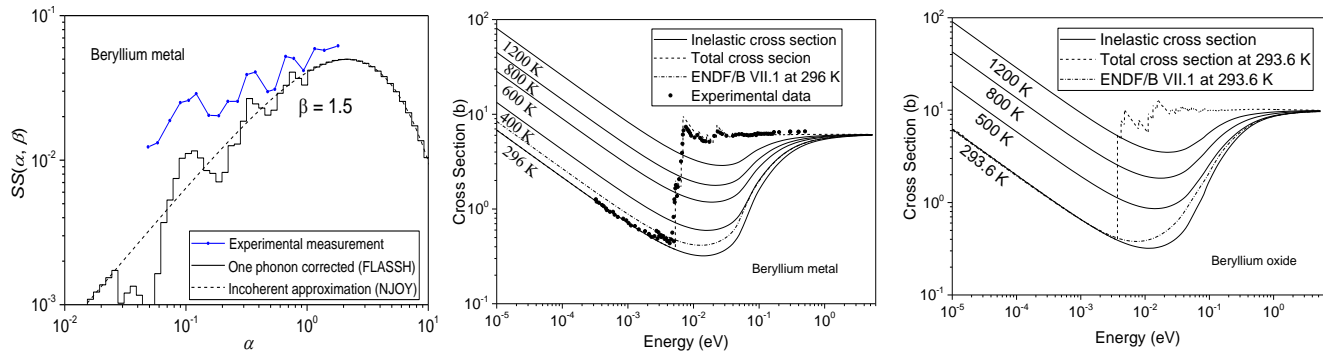
Fig. 2. The *ab initio* based TSL of beryllium metal, using Eq. 2 (NJOY's incoherent approximation) and the corrected result using Eq. 3, using the FLASSH code (left). The results obtained using Eq. 3 show improved agreement with experimental data. Also shown are the integral thermal inelastic scattering cross sections of beryllium metal (center) and beryllium oxide (right) calculated on the basis of Eq. 2. The calculated data shows good agreement with experimental data [14,17].
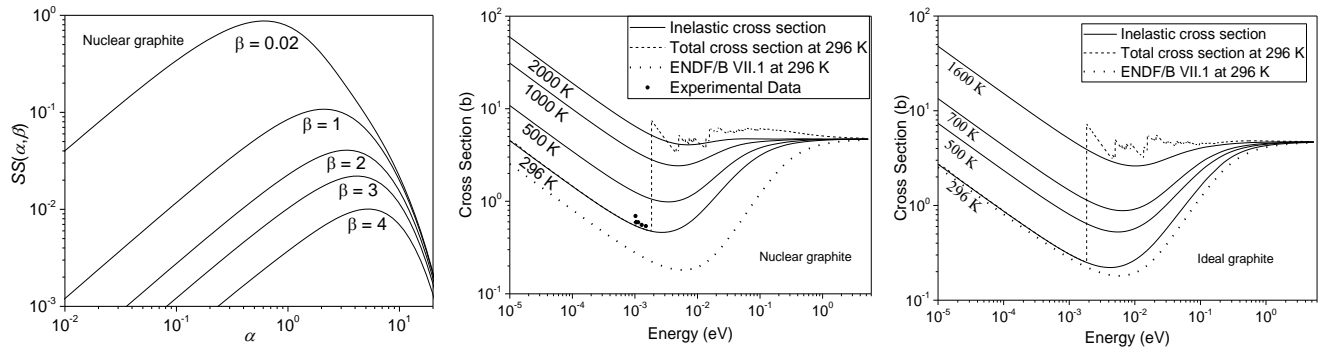
Fig. 3. The TSL of nuclear graphite at a porosity level of 10% and for a temperature of 300 K (left). The integral thermal inelastic scattering cross sections for nuclear graphite at various temperatures (center). Also shown is a comparison of the integral thermal inelastic scattering cross section of nuclear graphite to ideal (ENDF/B-VII) graphite. Nuclear graphite shows improved agreement with experimental data [14,15]. The integral thermal inelastic scattering cross sections for ideal graphite at various temperatures (right).